PCCP

Dynamic Article Links

Cite this: *Phys. Chem. Chem. Phys.*, 2012, **14**, 9929–9935

www.rsc.org/pccp

PAPER

UV photodesorption of interstellar CO ice analogues: from subsurface excitation to surface desorption

Mathieu Bertin,*[a] Edith C. Fayolle,[b] Claire Romanzin,[c] Karin I. Öberg,[d] Xavier Michaut,[a] Audrey Moudens,[a] Laurent Philippe,[a] Pascal Jeseck,[a] Harold Linnartz[b] and Jean-Hugues Fillion[a]

Received 12th April 2012, Accepted 14th May 2012
DOI: 10.1039/c2cp41177f

Carbon monoxide is after H_2 the most abundant molecule identified in the interstellar medium (ISM), and is used as a major tracer for the gas phase physical conditions. Accreted at the surface of water-rich icy grains, CO is considered to be the starting point of a complex organic – presumably prebiotic – chemistry. Non-thermal desorption processes, and especially photodesorption by UV photons, are seen as the main cause that drives the gas-to-ice CO balance in the colder parts of the ISM. The process is known to be efficient and wavelength-dependent, but, the underlying mechanism and the physical–chemical parameters governing the photodesorption are still largely unknown. Using monochromatized photons from a synchrotron beamline, we reveal that the molecular mechanism responsible for CO photoejection is an indirect, (sub)surface-located process. The local environment of the molecules plays a key role in the photodesorption efficiency, and is quenched by at least an order of magnitude for CO interacting with a water ice surface.

Introduction

In cold and dense interstellar regions, *i.e.* circumstellar clouds, protostellar envelopes and protoplanetary disks, molecules collide with and stick to (sub)micron-sized silicate and carbonaceous particles, resulting in icy mantles.[1] The two most abundant species found on icy dust grains in space are CO and H_2O.[2–4] From observational ice mapping and from spectroscopic details of CO infrared features, it has been concluded that the H_2O ice layer forms first on the grain and that most CO ice is present on top of the H_2O ice (*e.g.* ref. 5 and 6). The resulting balance of molecules in the solid state and in the gas phase is determined by freeze-out and sublimation, and specifically the CO ice–gas balance is of great interest for several reasons. First, gas phase CO is the most commonly used tracer of density and temperature in astrophysical environments. Therefore, accurate information on conditions under which CO can be found in the gas phase is vital to interpret such observations.[7,8] Second, CO ice is seen as the precursor of CH_3OH in space, which in its turn is the proposed starting point of a rich extra-terrestrial organic chemistry with possible ties to the origins of life.[9–12] Consequently, third, the exact location of CO freeze-out in the protoplanetary disks is proposed to affect the composition of exoplanets.[13]

Ice sublimation can occur through both thermal[14] and non-thermal desorption processes, and which process is finally determining the ice–gas balance depends on the temperature and radiation or particle flux. Astrophysical environments contain vacuum UV photons, cosmic-rays, and/or electrons, which all have the potential to induce ice sublimation and thus contribute to the gas-to-ice balance (*e.g.* ref. 15). Non-thermal desorption is expected to be especially important in cold regions ($T < 20$ K), where thermal effects are negligible; observations of rotationally cold gas-phase CO in such regions suggest the presence of an efficient non-thermal desorption process.[16,17] In order to quantify and model non-thermal sublimation for ices exposed to astrophysical flux levels and astronomical time scales, these processes must be understood at a molecular level. In this study we focus on vacuum UV photodesorption of CO ice, the proposed dominating non-thermal desorption process in most interstellar environments.[18]

The UV photodesorption of CO ice has been investigated in the laboratory in a number of studies using thin physisorbed CO ice films at temperatures between 10 and 25 K, irradiated by photons from broad-band H_2 discharge lamps peaking at 10.2 eV (Lyman-α). These studies have provided important empirical constraints: CO photodesorption is an efficient zeroth-order process, which depends on the ice temperature and seems confined to the ice surface or top few ice layers.[19–21]

[a] *UPMC Univ. Paris 6, Laboratoire de Physique Moléculaire pour l'Atmosphère et l'Astrophysique (LPMAA) – CNRS UMR 7092, F-75252 Paris, France. E-mail: mathieu.bertin@upmc.fr*
[b] *Sackler Laboratory for Astrophysics, Leiden Observatory, Leiden University, P.O. Box 9513, NL-2300 RA Leiden, The Netherlands*
[c] *Université Paris Sud 11, Laboratoire de Chimie Physique (LCP) – CNRS UMR 8000, F-91400 Orsay, France*
[d] *Harvard-Smithsonian Center for Astrophysics, 60 Garden Street, Cambridge, MA 02138, USA*

More recently, we carried out a pilot study to investigate the photon energy dependence of the CO photodesorption yields.[22] In those experiments synchrotron radiation was used to irradiate a CO ice with energies between 7 and 14 eV, the relevant UV range for star-forming regions, while monitoring the amount of CO photodesorbed in the gas phase. These measurements demonstrated that the UV photodesorption of CO ice is highly wavelength dependent and directly correlated with the electronic absorption spectrum of the ice, suggesting that desorption is induced by electronic transition (DIET). Monochromatic ice photodesorption studies are thus a potentially powerful technique to probe the underlying molecular sublimation mechanism.

In the present work we build on the technical developments and preliminary results available from the pilot study to obtain the first comprehensive view of the CO ice UV photodesorption process. The ultimate goal is a full mechanistic understanding, and this requires resolving the location of the relevant excitation process, determining the role of the substrate, and constraining whether excited molecules desorb themselves or distribute energy to neighboring CO molecules, resulting in an indirect desorption mechanism. Disentangling the role of the substrate and which parts of the ice are photodesorption-active are key issues that need to be addressed to accurately extrapolate the laboratory results to astronomical boundaries.

In the present paper, narrowband tunable UV radiations from the DESIRS synchrotron beamline and state-of-the-art surface science techniques are used to probe the photodesorption mechanism at a molecular level, highlighting new key-parameters that drive the efficiency of the process. Especially, different local CO environments, mimicking realistic conditions in interstellar ices (pure CO ice or CO interacting with water), are shown to have a dramatic effect on the photodesorption efficiency.

Methods

The CO ices photodesorption study is realized in the 'SPICES' (Surface Processes & ICES) setup of the UPMC (Université Pierre et Marie Curie). Molecular ices (CO and/or H_2O) of various thicknesses are grown with monolayer precision under ultrahigh vacuum (UHV) conditions ($P < 5 \times 10^{-10}$ Torr) on a highly oriented pyrolitic graphite (HOPG) or a polycrystalline gold substrate. The two substrates are mounted on opposite sides of the tip of a turnable coldhead that is cooled down to 14 K by a closed cycle helium cryostat. The ice layers are grown by diffuse deposition of CO gas (Air Liquide, 99% purity) or H_2O vapour (high purity, liquid chromatography standard from Fluka) and the setup allows for accurate growth of different isotopic layers on top of each other. The quantities of molecules deposited on the substrate are expressed in ML_{eq} or BL_{eq} (mono/bilayer equivalents for CO and H_2O, respectively) corresponding to the density of a compact molecular layer on a flat surface, with $1\ ML_{eq} \approx 1\ BL_{eq} \approx 1 \times 10^{15}$ molecule per cm^2.[23,24]

The Temperature Programmed Desorption (TPD) method is used for the calibration of the ice thicknesses, resulting in reproducible parameters for the growth conditions with a $1\ ML_{eq}$ precision. This technique is also employed to characterize the CO adsorption onto amorphous or crystalline water ices. The shape and position of the desorption peaks are related to CO desorption from (i) pure CO multilayers, (ii) a CO monolayer interacting with the water surface, and (iii) CO trapped within the water ice, as already studied in ref. 23 and 25.

UV photodesorption is induced through irradiation of the CO ice sample by the continuous output of the undulator-based vacuum UV DESIRS beamline of the synchrotron SOLEIL,[26] providing photons whose energy can be continuously scanned over the 7 to 14 eV range. A narrow bandwidth of typically 40 meV is selected by the 6.65 m normal incidence monochromator implemented in the beamline. A specific gas filter equipping the beamline suppresses the high harmonics of the undulator that could be transmitted by the grating higher orders of diffraction. The absolute incident photon flux impinging onto the sample, measured by a calibrated photodiode, is about 10^{12} photons per s. The UHV setup and the beamline are directly connected, without any window, in order to prevent radiation cut-off.

The photodesorption spectra are recorded in real time, *i.e.* during ice irradiation, monitoring the gas phase composition by means of a Quadrupole Mass Spectrometer (QMS). The desorption rate per incident photon is derived from the resulting Photon-Stimulated Desorption (PSD) spectra and the measured energy-dependent photon flux.[22] In the presented PSD spectra, the photon energy is automatically scanned from 7 to 14 eV with steps of 25 meV. Each energy step lasts $\sim$5 s. In the mean time, the QMS signal is recorded with a dwell of 1 s, which makes an average of 5 points per energy step. Caution has been taken so that, for each point, the 1 s accumulation time is much longer than the QMS mass signal build-up time, thus preventing artefacts due to the energy scan speed. Indeed, it has been verified that changing the scanning speed does not lead to a modification of the mass signal–energy correlation in the PSD spectra.

Simultaneously, the composition of the condensed phase can be monitored using Fourier Transform Reflection Absorption Infrared Spectroscopy (FT-RAIRS). At the relatively low doses used, no newly formed species has been observed during the irradiations regardless of ice (pure CO or H_2O–CO ices), neither in the condensed phase nor in the gas phase. Therefore, chemistry is not expected to play a measurable role in our PSD experiments. More experimental details on the used UHV setup 'SPICES' are available from ref. 27 and the use of SOLEIL/DESIRS as a VUV light source from ref. 28.

Results and discussion

Pure CO ice desorption – an exclusive DIET process

Fig. 1 presents the Photon Stimulated Desorption spectra of pure CO ices deposited on polycrystalline gold (Fig. 1a) and Highly Oriented Pyrolitic Graphite (HOPG) (Fig. 1b) at 14 K at ice thicknesses from 3 to 250 ML_{eq}. The spectra are obtained by recording the mass signal of desorbing CO in the gas phase while irradiating a pure CO ice with UV light continuously tuned from 7 to 14 eV. From this, the CO photodesorption rate is derived as a function of the energy of the incident photons. In agreement with Fayolle *et al.*,[22] the CO photodesorption rate is found to be strongly wavelength-dependent, and to follow below 10.5 eV the UV absorption spectrum of condensed CO.[29] The observed pattern is due to

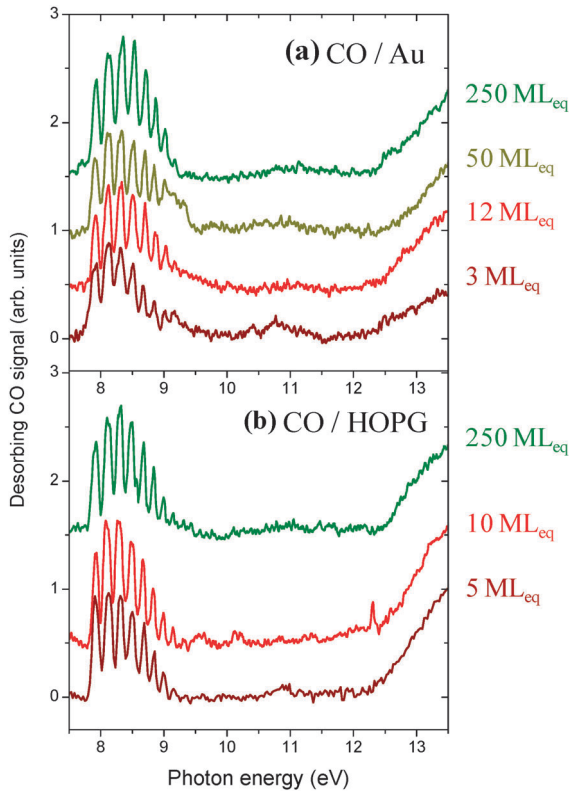

Fig. 1 Photon-Stimulated Desorption (PSD) spectra for several thicknesses of pure CO ice deposited at 14 K on top of (a) a polycrystalline gold or (b) a highly oriented pyrolitic graphite (HOPG) surface.

the vibronic progression of the transition from the electronic $X^1\sum^+$ ($v = 0$) ground state to the first dipole-allowed excited electronic state $A^1\Pi$ ($v' = 0, 1, 2, \ldots$) of the condensed CO molecules. The recorded PSD spectrum, logically, indicates that photodesorption is triggered by an electronic excitation within the molecular ice. Since the first electronically excited $A^1\Pi$ level is a non-dissociative state,[30,31] desorption triggered by the fragmentation of CO can be excluded. Thus, the desorption process must occur *via* a direct transfer of absorbed energy, in which the electronic excitation energy is redistributed to intra- or intermolecular vibrational modes that provide the kinetic energy for the CO ejection. This mechanism is known as a DIET process (Desorption Induced by Electronic Transition).[32–34]

DIET may not be acting exclusively, however. In particular, UV-induced substrate-mediated processes may contribute – non-resonantly – to the overall CO photodesorption rate. Photoelectrons originating from the substrate may trigger CO desorption through electronic excitation or electron attachment.[34–36] UV-induced electron–hole pairs also can contribute to the CO desorption through a strong electron–phonon coupling.[37,38] Because all these processes involve the substrate–ice interface, the potential contribution from these processes to the overall photodesorption rate is expected to be different for different substrate surfaces, and to be less prominent for thick CO ice coverage, since the number of photons reaching the substrate decreases due to absorption by the above-lying ice. Fig. 1a and b show that the wavelength response and intensity of the photodesorption spectra are identical for the HOPG and gold surface and that there is no thickness dependency for coverages exceeding 3 ML$_{eq}$. This rules out that the substrate contributes substantially to the measured photodesorption rates and confirms that CO photodesorption is thus an exclusive DIET process.

Subsurface excitation

The use of different ice thicknesses allows us to constrain the ice region directly associated with the photodesorption events; Fig. 1 shows that CO photodesorption is equally efficient – within a relative spread of 5% of the desorption signal – for ice coverages over two orders of magnitude, from 250 ML$_{eq}$ down to 3 ML$_{eq}$. This implies that only the topmost ice layers are involved in the photodesorption process.

To further localize the photodesorption process, vacuum UV photodesorption experiments are performed on layered and isotopically labeled CO ices, comprising thin layers of ^{13}CO ice, deposited at different thicknesses on top of a 10 ML$_{eq}$ thick ^{12}CO ice. PSD spectra of desorbing ^{12}CO (28 amu, Fig. 2a) and ^{13}CO (29 amu, Fig. 2b) directly reveal from which ice layers molecules are photodesorbed. In the experiments, 1 ML$_{eq}$ of ^{13}CO deposited on ^{12}CO reduces the ^{12}CO desorption yield, but does not completely quench it, and a strong ^{13}CO signal is observed. The addition of a second layer of ^{13}CO largely blocks all ^{12}CO desorptions, while the ^{13}CO desorption rate becomes comparable to that of ^{12}CO from 10 ML$_{eq}$ pure ^{12}CO ice. Only molecules from the two topmost layers are thus photodesorbed.

These results do not necessarily imply, however, that the actual excitation process resulting in a photodesorption event only involves molecules in the top two ice layers. Complementary information on the excitation process can be extracted from the details of the PSD spectra; the peak positions in the PSD spectrum for different ^{13}CO ice coverages between 7.5 and 10.5 eV presented in Fig. 2c (zoom-in of Fig. 2b) unveil precious information on the isotopologue location of the initial excitation step. For ^{13}CO coatings thinner than 2 ML$_{eq}$, the PSD spectrum matches the vibronic structure of the $A^1\Pi$ (v') $\leftarrow$ $X^1\sum^+$ ($v = 0$) electronic transition for condensed ^{12}CO.[29] The majority of the initial photon absorption events therefore must take place in the underlying ^{12}CO ice and not in the isotopic top layer, from which the photodesorbing molecules originate; the excess energy deposited in the ^{12}CO is transferred to the surface ^{13}CO molecules. This is an indication that CO ice photodesorption is an indirect process where surface molecules are desorbed second to electronic excitation of sub-surface molecules.

When the ^{13}CO cover layer exceeds 3 ML$_{eq}$, the spectral signature partially changes, as can be seen from the decrease in higher vibrational level spacings (Fig. 2c). Obviously transitions involving high v' vibrational levels in the upper electronic state are red shifted. Such a behaviour is expected in the case of a heavier isotopologue excitation (^{13}CO compared to ^{12}CO), and should therefore be associated with the excitation of the $^1\Pi$ (v') levels of the condensed ^{13}CO. Indeed, the obtained PSD spectrum becomes identical to the PSD spectrum of a pure 20 ML$_{eq}$ ice of ^{13}CO.

As 3 ML$_{eq}$ of ^{13}CO are needed to observe ^{13}CO-related absorption features, it is likely that the initial excitation step occurs within the 2 to 3 topmost molecular layers. UV absorption in the top ice layer does not efficiently result in a photodesorption event;

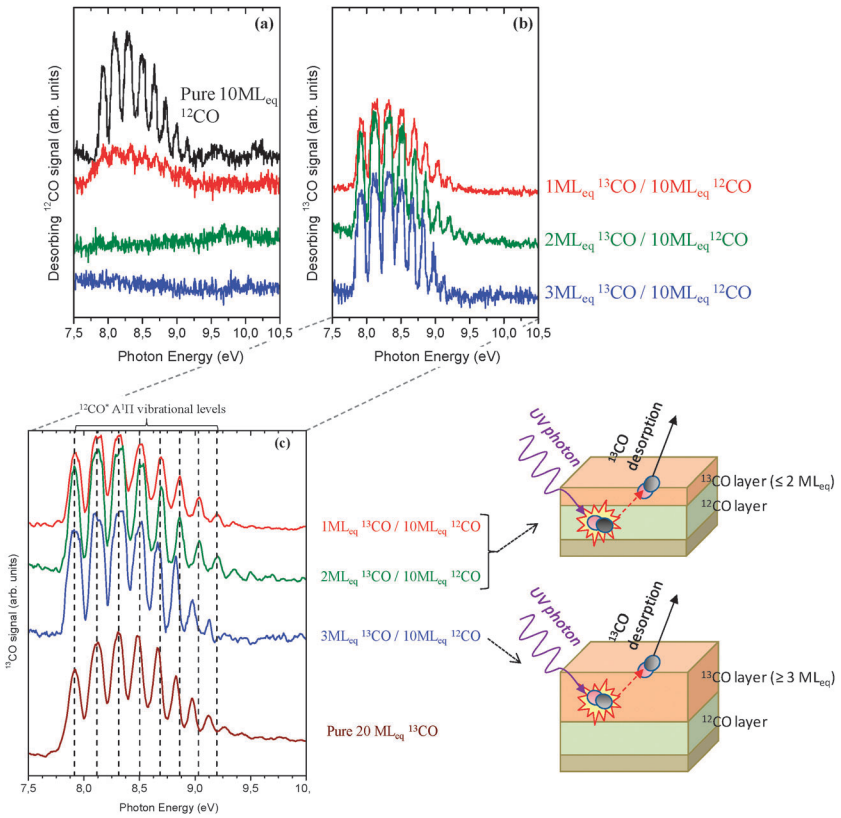

Fig. 2 ^{12}CO (a) and ^{13}CO (b) photon stimulated desorption spectra at 14 K of 10 ML$_{eq}$ ^{12}CO ice, covered with a layer of increasing thickness of ^{13}CO. The panel (c) shows a zoom-in of the ^{13}CO PSD spectra on the ^{13}CO/^{12}CO layered ice compared to the one obtained on a pure ^{13}CO ice at 14 K. The dashed lines correspond to the energies of the first vibronic levels in a pure ^{12}CO ice from ref. 29.

rather CO UV photodesorption is a three-step process at the investigated UV frequencies. This is schematically depicted in Fig. 3: (i) a subsurface-located CO molecule absorbs a UV photon and gets electronically excited, (ii) the internal excess energy of the excited molecule gets partly transferred to a surface-located CO molecule *via* the excitation of intermolecular vibrational modes, providing sufficient energy to (iii) eject a surface molecule into the gas phase.

This finding of an indirect DIET mechanism has important consequences concerning the carbon monoxide UV-photodesorption on interstellar grains, since it implies that the presence of other species interacting with CO molecules can potentially perturb, or even quench, the intermolecular energy transfer mechanism. This effect has therefore been tested here experimentally by determining the photodesorption efficiency of the astronomically relevant scenario of CO ices deposited on top of water ice.

Photodesorption of solid CO on top of H_2O ice

The CO photodesorption yield from top of H_2O ice provides an important complementary check for the proposed indirect DIET mechanism. As mentioned before CO ice in the interstellar medium is mainly found on top of H_2O-ice-coated dust grains, where it may be involved in chemical processes leading to H_2CO or CH_3OH formation. The thickness of this ice layer varies substantially, and ice observations using the Very Large Telescope (VLT) conclude that in space CO is both present in a pure CO ice phase, and in a phase that is strongly interacting

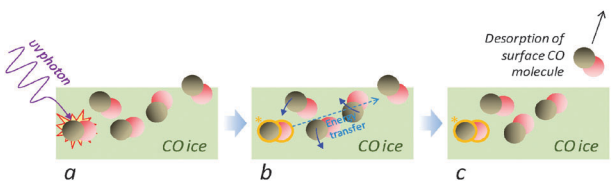

Fig. 3 Scheme of the CO photodesorption three-step mechanism: (a) a UV photon is absorbed in the subsurface region of the CO ice, promoting a molecule into its A^{1}Π electronic state, (b) the neighbouring CO rearrange around the excited molecule, resulting in the excitation of intermolecular vibrational modes, and (c) a surface CO molecule receives enough kinetic energy to be ejected from the ice.

through hydrogen bonding, presumably with the water molecules of the underlying ice.[5,39] The two relevant photodesorption yields that need to be experimentally characterized are thus from pure CO ices, and from CO layers on top of H_2O.

From the pure CO ice experiments, CO ices thicker than 2 layers are expected to desorb following a DIET indirect process, and it is unclear whether this indirect process will work if the CO molecules are interacting with subsurface H_2O in addition to other CO molecules. In order to address this question, PSD experiments of CO ice on top of H_2O have been performed using the same experimental techniques introduced for the pure ice experiments. Fig. 4 shows PSD spectra for different CO ice thicknesses, deposited at 14 K on top of 250 BL$_{eq}$ water ice films. Two different water ice phases have been investigated: an amorphous porous ice, prepared at 14 K (Fig. 4a), and a

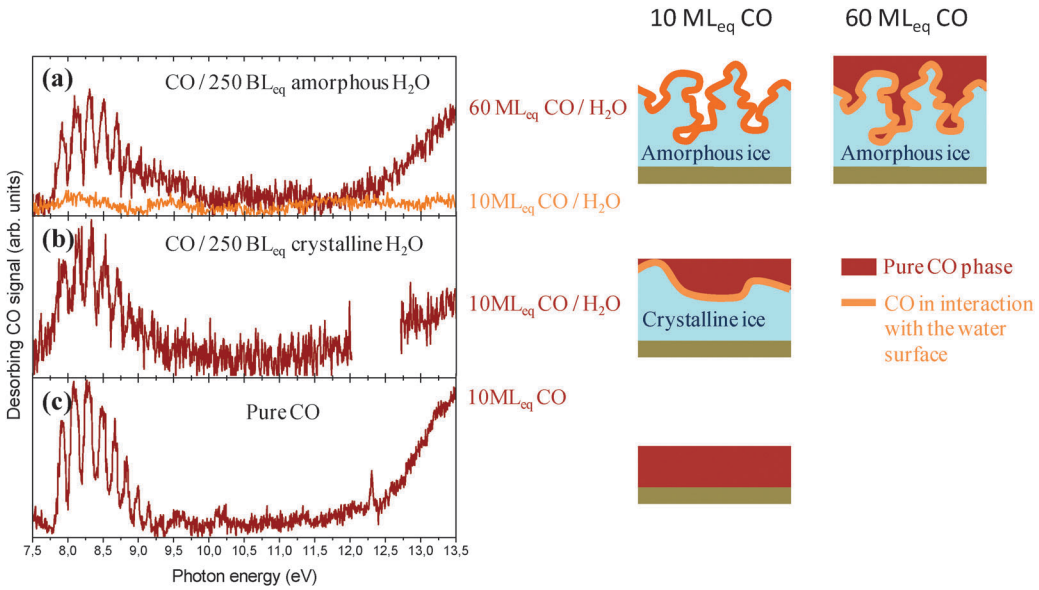

Fig. 4 Photon stimulated desorption spectra for different amounts of CO deposited on (a) amorphous water ice, (b) polycrystalline water ice, and (c) HOPG at 14 K. The corresponding ice morphologies are schematically depicted. The CO desorption is only observed when a pure CO phase is grown upon deposition.

polycrystalline ice, grown at 140 K (Fig. 4b). Fig. 4a shows that no CO photodesorption can be observed for irradiating photon energies between 7 and 14 eV from 10 ML$_{eq}$ CO on top of amorphous water ice. For a substantially thicker coating of 60 ML$_{eq}$ CO ice layer on top of the same water ice, the photodesorption spectrum is almost identical to the PSD spectrum of pure CO ice (Fig. 4c). Obviously, the water layer can affect the CO photodesorption yield.

Due to the very large specific surface of amorphous H_2O, a large amount of the CO molecules are needed to saturate the ice–vacuum interface of the water ice.[14,23,25] Using studies performed by Collings *et al.*,[23,25] we evidenced from thermal desorption experiments that 10 ML$_{eq}$ of CO are clearly below the amount of molecules needed to totally recover the available surface of the amorphous water ice. As a consequence, all molecules in the 10 ML$_{eq}$ of deposited CO interact directly with the H_2O molecules, and no pure solid CO ice is grown upon deposition. This is not the case anymore when 60 ML$_{eq}$ of CO molecules are deposited on top of amorphous porous H_2O: the water specific surface is saturated, and $\sim$3 ML$_{eq}$ of a pure CO phase, *i.e.* multilayer of CO, grows on top of the amorphous H_2O ice. From this finding, it is concluded that a pure CO phase is needed for the photodesorption to be effective.

This model is confirmed by the experiments on polycrystalline water ice. Indeed, for the same coverage the effective surface of the compact and ordered crystalline ice is much smaller than the disorganized and porous amorphous ice film surface, and the higher compactness of the ice prevents CO to penetrate in an equally efficient way as for the amorphous morphology.[40–43] 10 ML$_{eq}$ of CO are therefore a sufficient coverage to achieve a CO multilayer phase. As clearly observed from Fig. 4b, this phase is photodesorption-active, following the same indirect DIET process as found in the case of a pure CO ice.

The lack of observed photodesorption for CO molecules interacting with H_2O is consistent with the proposed indirect DIET mechanism. These CO molecules are located in the vicinity of the water surface, which allows either subsurface CO photoexcitation or H_2O photoexcitation/dissociation to be the first step in the photodesorption mechanism as also water ice absorbs in the 7–14 eV energy range.[44,45] The second step requires (i) the subsequent excitation of intermolecular modes and (ii) the energy transfer towards a surface CO molecule. These steps are expected to be strongly perturbed by the presence of the water, because of the very different nature of the intermolecular interactions compared to pure solid CO; the hydrogen bridged H_2O–CO interactions are stronger than pure van der Waals interactions in solid CO, and it has recently been shown that dangling O–H bonds of surface H_2O present a unique ability to rapidly and efficiently evacuate excess vibrational energy from the surface to the bulk.[46] This opens an additional relaxation pathway that competes with the intermolecular energy transfer to a surface CO molecule. Finally, in the third step, the ejection of the CO molecule, the very high corrugation of the amorphous H_2O ice may block a sublimation event; a photodesorbed CO molecule can collide with the 14 K structured water surface, and be re-trapped before being emitted into the vacuum. UV induced photochemistry at the H_2O–CO interface could play a role in the observed lack of desorption too, but this effect should be minor, since neither infrared spectroscopy nor mass spectrometry has revealed the presence of new chemical species in our experiments.

In astrophysical environments the UV photodesorption yield is thus expected to be substantially different for thick and thin CO ices on top of H_2O. In regions where icy grains are covered with multilayers of pure CO ice, the UV photodesorption is an efficient process,[19–22] depending on the wavelength of the incoming radiation, and it is a plausible explanation for the observations of gas phase CO molecules in regions with temperatures below the accretion temperature of CO.

The laboratory work presented here shows that this process is heavily suppressed at the CO–H_2O ice interface. The environment of the CO molecule in an interstellar ice governs its photodesorption efficiency, which needs to be taken into account when modeling the CO gas–ice balance in interstellar environments. From our PSD spectra in the 7–14 eV energy range and our detection limit, we estimate that the CO photodesorption yield is reduced by a factor of 15, at least, for the CO–H_2O system as compared to the pure CO multilayer film.

Conclusions

The wavelength-dependent photon stimulated desorption methods presented here offer a powerful tool to explore molecular processes involved in the photodesorption of interstellar ices. While the wavelength dependence of the desorption process allows an absolute photodesorption rate, applicable to any UV field spectrum, to be derived,[22] it also provides valuable information on the underlying CO desorption molecular mechanism. Our studies show that the photodesorption mechanism of CO ice involves only the top-most molecular layers of the solid, and does not depend on the substrate onto which the ice is grown. Rather, the mechanism is a three-step indirect DIET process, in which the intermolecular interactions between the CO surface and sub-surface molecules govern the desorption efficiency. This last point has important consequences for the photodesorption of CO in interstellar ices. It is known from observational studies that, in the ISM, one part of the CO molecules forms a pure CO phase layer on top of water-rich icy grains, while the other part is involved in hydrogen-bound complexes with water molecules. From our finding we conclude that at least 2 pure CO layers are needed for the photodesorption process to be effective. In contrast, the efficiency of the photodesorption of CO molecules interacting with water ice surfaces is found to be reduced by at least a factor of 15 compared to pure CO ices. The presented indirect DIET mechanism implies that CO molecules interacting with the water molecules do not photodesorb efficiently, while pure CO ice molecules do.

Acknowledgements

We acknowledge the SOLEIL general staff for running the synchrotron radiation facility, and we would like to thank Dr L. Nahon and his team for assistance in using beamline DESIRS under the project no. 20110013. We gratefully acknowledge Prof. M. van Hemert for very fruitful discussions on the CO photodesorption mechanisms, and P. Marie-Jeanne for technical support on the SPICES experimental setup. M.B., X.M., L.P., C.R., P.J., A.M. and J.-H.F. acknowledge financial support from the French national program PCMI (Physique et Chimie du Milieu Interstellaire). A.M. is financially supported by the French National Agency for Research (ANR) under the contract number ANR-09-BLAN-0066-01. The research in Leiden is supported by NOVA (Nederlandse Onderzoekschool Voor Astronomie), NWO-VICI and LASSIE, a European FP7 ITN Community's Seventh Frameword Program under Grant Agreement no. 238258. The authors thank support from the Hubert Curien Partnership 'Van Gogh' – project no. 25055YK. Support for K.I.Ö. is provided by NASA through the Hubble Fellowship grant awarded by the Space Telescope Science Institute, which is operated by the Association of Universities for Research in Astronomy, Inc., for NASA, under contract NAS 5-26555.

Notes and references

1 A. G. G. M. Tielens and W. Hagen, *Astron. Astrophys.*, 1982, **114**, 245–260.
2 F. C. Gillett and W. J. Forrest, *Astrophys. J.*, 1973, **179**, 483–491.
3 E. Dartois, *Space Sci. Rev.*, 2005, **119**, 293–310.
4 K. I. Öberg, A. C. A. Boogert, K. M. Pontoppidan, S. van den Broek, E. F. van Dishoeck, S. Bottinelli, G. A. Blake and N. J. Evans II, *Astrophys. J.*, 2011, **740**, 109.
5 K. M. Pontoppidan, A. C. A. Boogert, H. J. Fraser, E. F. van Dishoeck, G. A. Blake, F. Lahuis, K. I. Öberg, N. J. Evans and C. Salyk, *Astrophys. J.*, 2008, **678**, 1005–1031.
6 H. M. Cuppen, E. M. Penteado, K. Isokoski, N. van der Marel and H. Linnartz, *Mon. Not. R. Astron. Soc.*, 2011, **417**, 2809–2816.
7 E. A. Bergin, D. R. Ciardi, C. J. Lada, J. Alves and E. A. Lada, *Astrophys. J.*, 2001, **557**, 209–225.
8 C. Qi, D. J. Wilner, N. Calvet, T. L. Bourke, G. A. Blake, M. R. Hogerheijde, P. T. P. Ho and E. Bergin, *Astrophys. J. Lett.*, 2006, **636**, L157–L160.
9 G. W. Fuchs, H. M. Cuppen, S. Ioppolo, C. Romanzin, S. E. Bisschop, S. Andersson, E. F. van Dishoeck and H. Linnartz, *Astron. Astrophys.*, 2009, **505**, 629–639.
10 K. I. Öberg, R. T. Garrod, E. F. van Dishoeck and H. Linnartz, *Astron. Astrophys.*, 2009, **504**, U891–U913.
11 N. Watanabe and A. Kouchi, *Astrophys. J. Lett.*, 2002, **571**, L173–L176.
12 E. Herbst and E. F. van Dishoeck, in *Annual Review of Astronomy and Astrophysics*, Annual Reviews, Palo Alto, 2009, vol. 47, pp. 427–480.
13 K. I. Öberg, R. Murray-Clay and E. A. Bergin, *Astrophys. J. Lett.*, 2011, **743**, L16.
14 D. J. Burke and W. A. Brown, *Phys. Chem. Chem. Phys.*, 2010, **12**, 5947–5969.
15 C. J. Shen, J. M. Greenberg, W. A. Schutte and E. F. van Dishoeck, *Astron. Astrophys.*, 2004, **415**, 203–215.
16 V. Piétu, A. Dutrey and S. Guilloteau, *Astron. Astrophys.*, 2007, **467**, 163–178.
17 A. Oka, T. Nakamoto and S. Ida, *Astrophys. J.*, 2011, **738**, 141.
18 K. Willacy and W. D. Langer, *Astrophys. J.*, 2000, **544**, 903–920.
19 G. M. Muñoz Caro, A. Jimenez-Escobar, J. A. Martin-Gago, C. Rogero, C. Atienza, S. Puertas, J. M. Sobrado and J. Torres-Redondo, *Astron. Astrophys.*, 2011, **522**, 14.
20 K. I. Öberg, G. W. Fuchs, Z. Awad, H. J. Fraser, S. Schlemmer, E. F. Van Dishoeck and H. Linnartz, *Astrophys. J.*, 2007, **662**, L23–L26.
21 K. I. Öberg, E. F. van Dishoeck and H. Linnartz, *Astron. Astrophys.*, 2009, **496**, 281–293.
22 E. C. Fayolle, M. Bertin, C. Romanzin, X. Michaut, K. I. Öberg, H. Linnartz and J.-H. Fillion, *Astrophys. J. Lett.*, 2011, **739**, L36.
23 M. P. Collings, J. W. Dever, H. J. Fraser and M. R. S. McCoustra, *Astrophys. Space Sci.*, 2003, **285**, 633–659.
24 D. V. Chakarov, L. Osterlund and B. Kasemo, *Langmuir*, 1995, **11**, 1201–1214.
25 M. P. Collings, J. W. Dever, H. J. Fraser, M. R. S. McCoustra and D. A. Williams, *Astrophys. J.*, 2003, **583**, 1058–1062.
26 DESIRS, Beamline website: http://www.synchrotron-soleil.fr/portal/page/portal/Recherche/LignesLumiere/DESIRS.
27 M. Bertin, C. Romanzin, X. Michaut, P. Jeseck and J. H. Fillion, *J. Phys. Chem. C*, 2011, **115**, 12920–12928.
28 L. Nahon, N. de Oliveira, G. A. Garcia, J.-F. Gil, B. Pilette, O. Marcouillé, B. Lagarde and F. Polack, *J. Synchrotron Radiat.*, 2012, DOI: 10.1107/S0909049512010588.
29 H. C. Lu, H. K. Chen, B. M. Cheng, Y. P. Kuo and J. F. Ogilvie, *J. Phys. B: At., Mol. Opt. Phys.*, 2005, **38**, 3693–3704.
30 H. Okabe, *Photochemistry of small molecules*, Wiley Interscience, New York, 1978.
31 H. Cottin, M. H. Moore and Y. Benilan, *Astrophys. J.*, 2003, **590**, 874–881.

32 P. Avouris and R. E. Walkup, *Annu. Rev. Phys. Chem.*, 1989, **40**, 173–206.
33 D. Bejan, *J. Optoelectron. Adv. Mater.*, 2004, **6**, 359–384.
34 O. Rakhovskaia, P. Wiethoff and P. Feulner, *Nucl. Instrum. Methods Phys. Res., Sect. B*, 1995, **101**, 169–173.
35 A. Mann, P. Cloutier, D. Liu and L. Sanche, *Phys. Rev. B: Condens. Matter Mater. Phys.*, 1995, **51**, 7200–7206.
36 H. Shi, P. Cloutier and L. Sanche, *J. Low Temp. Phys.*, 1998, **24**, 742–747.
37 M. Bonn, S. Funk, C. Hess, D. N. Denzler, C. Stampfl, M. Scheffler, M. Wolf and G. Ertl, *Science*, 1999, **285**, 1042–1045.
38 S. Funk, M. Bonn, D. N. Denzler, C. Hess, M. Wolf and G. Ertl, *J. Chem. Phys.*, 2000, **112**, 9888–9897.
39 K. M. Pontoppidan, H. J. Fraser, E. Dartois, W. F. Thi, E. F. van Dishoeck, A. C. A. Boogert, L. d'Hendecourt, A. Tielens and S. E. Bisschop, *Astron. Astrophys.*, 2003, **408**, 981–1007.
40 B. Rowland, M. Fisher and J. P. Devlin, *J. Chem. Phys.*, 1991, **95**, 1378–1384.
41 K. P. Stevenson, G. A. Kimmel, Z. Dohnalek, R. S. Smith and B. D. Kay, *Science*, 1999, **283**, 1505–1507.
42 Z. Dohnalek, R. L. Ciolli, G. A. Kimmel, K. P. Stevenson, R. S. Smith and B. D. Kay, *J. Chem. Phys.*, 1999, **110**, 5489–5492.
43 G. A. Kimmel, K. P. Stevenson, Z. Dohnalek, R. S. Smith and B. D. Kay, *J. Chem. Phys.*, 2001, **114**, 5284–5294.
44 R. Mota, R. Parafita, M. J. P. Maneira, N. J. Mason, G. Garcia, P. A. Ribeiro, M. Raposo and P. Limao-Vieira, *Radiat. Prot. Dosim.*, 2006, **122**, 66–71.
45 N. J. Mason, A. Dawes, P. D. Holtom, R. J. Mukerji, M. P. Davis, B. Sivaraman, R. I. Kaiser, S. V. Hoffmann and D. A. Shaw, *Faraday Discuss.*, 2006, **133**, 311–329.
46 Z. Zhang, L. Piatkowski, H. J. Bakker and M. Bonn, *Nat. Chem.*, 2011, **3**, 888–893.